Polish J. Chem., **75**, 1417–1425 (2001)

New Molecular Composites: Pyridine Derivatives as Guest Molecules Encapsulated within the Cavities of the Three-Dimensional Supramolecular Complexes – $[(R_3Sn)_3Fe(CN)_6]_n$, R = Ph or n-Bu

by M.Sh. Ibrahim* and S.H. Etaiw

Chemistry Department, Faculty of Science, University of Tanta, Tanta, Egypt

(Received January 5th, 2001; revised manuscript June 5th, 2001)

Spontaneous self assembly reaction of $[-Fe(CN)_6]^{3-}$ building blocks and R_3Sn^+ ions (R = alkyl or aryl) affords three-dimensional (3D) supramolecular $[(R_3Sn)_3Fe(CN)_6]_n$ products, which were confirmed by different spectral data. The architecture of these supramolecular complexes involve guest-free cyanide-bridged 3D neutral networks. They are composed of nearly plannar R_3Sn^+ units, linked together with slightly distorted octahedral building blocks $[-Fe(CN)_6]^{3-}$ through the cyanide N atoms. Pyridine compounds, acting as guest donors, have been successfully encapsulated within the expandable wide cavities of the 3D-supramolecular complexes by tribochemical reactions. This produces novel charge transfer molecular composites. The properties of the resulting molecular composites were investigated by elemental analyses, IR, UV-visible, X-ray powder diffraction, EPR and magnetic moments. The interesting feature of these molecular composites are their semiconductive properties.

Key words: 3D-host supramolecular complexes, pyridine compounds, molecular composites

The architecture of "super-prussian blue" and related compounds, $Ag_3[Co(CN)_6]$ and $Au_3[Co(CN)_6]$, should consist of three equivalent and independent frameworks with [-CN-M-NC-] (M = Ag or Au) instead of (CN) group connected between two metal ions [1]. A novel class of organometallic supramolecular complexes were obtained by the formal replacement of each Ag^+ or Au^+ ions by a planar R_3Sn^+ (R = alkyl or aryl) fragment as spacer. Various supramolecular complexes having the general formula $[(R_3Sn)_3M(CN)_6]_n = [M\{\mu\text{-}(CNSnR_3NC\}_3]_n$ have been prepared. The structure of these supramolecular complexes were confirmed by single-crystal structures of $[(Me_3E)_3Co(CN)_6]_n$ (E = Pb or Sn) [2,3], $[(Ph_3Sn)_3Fe(CN)_6]_n \cdot H_2O \cdot 2CH_3CN$ [4] and $[(n\text{-}Bu_3Sn)_3M(CN)_6]_n$ (M = Fe or Co) [5]. The octahedral building blocks $[-Fe(CN)_6]^{3-}$ are linked together through the trigonal bipyramidal (R_3Sn) connecting units, and remarkably wide parallel channels [3]. The oxidative properties of these supramolecular complexes can be demonstrated chemically by the facile encapsulation of voluminous organic or organometallic guest cations G^{n+} into negatively

*Author for correspondence.

charged host lattice $[(R_3Sn)_3Fe^{II}(CN)_6^-]_n$, formally by reduction of isostructural iron $[(R_3Sn)_3Fe^{III}(CN)_6]_n$ [6–8]. A large number of different Lewis bases including pyridine and pyridine derivatives have been successfully encapsulated into layered host materials, such as transition metal dichalcogenides and FeOCl by a guest-host redox reaction [9,10].

The present study develops the synthesis and characterization of new molecular composites by encapsulating pyridine compounds within the cavities of 3D $[(R_3Sn)_3Fe^{III}(CN)_6]_n$, (R = Ph or n-Bu), supramolecular complexes. The pyridine compounds, acting as electron donors, can be introduced quantitatively into the cavities of the 3D-supramolecular complexes acting as an electron acceptor. The elemental analyses, vibrational spectra, magnetic properties and electrical conductivity of the new molecular composites are discussed.

EXPERIMENTAL

Materials and preparations: All materials were of reagent grade and were used without purification. The host 3D-supramolecular complexes, $[(R_3Sn)_3Fe(CN)_6]_n$, (R = Ph or n-Bu), were prepared by mixing the organotin chloride and potassium hexacyanoferrate in water-acetone mixture in 3:1 molar ratio. The precipitates were filtered off, washed sequentially with water, acetone and diethylether, dried under vacuum at room temperature [3,11].

$$K_3[Fe(CN)_6] + 3\ R_3SnCl \rightarrow [(R_3Sn)_3Fe(CN)_6]_n + 3\ KCl;\ R = Ph\ \mathbf{I}\ or\ n\text{-}Bu\ \mathbf{II} \quad (1)$$

The purity and identity of **I** and **II** were checked by elemental analyses and vibrational spectra. New molecular composites were prepared under anhydrous conditions by adding the dry freshly prepared of **I** and **II** to an excess of the pyridine compounds, namely pyridine, 2-methylpyridine, 3-methylpyridine, 4-methylpyridine, 3-bromopyridine or 2-phenylpyridine with slight grinding. The colour products, **1–12**, were isolated, washed with ethanol to remove the unreacted materials, dried under vacuum at room temperature and their compositions were checked by elemental analyses.

Instruments: Elemental analyses were preformed on a Perkin Elmer 2400 automatic elemental analyzer. IR spectra were recorded as KBr discs in the range 4000–400 cm^{-1} using a Perkin Elmer sp 1430 spectrophotometer. UV/Vis absorption spectra were recorded on a Shimadzu 3101 pc spectrophotometer as nujol mull matrix. The solid powder EPR spectra were recorded on a JEOL spectrophotometer model JES-FE2XG. The magnetic susceptibility was determined with a Johnson-Matthey susceptometer. The X-ray powder diffraction pattern were recorded for CuKα radation using a Ni filter at room temperature. The electrical conductivities (Scm^{-1}) were measured by compressing the sample under a pressure of about 600 Kg cm^{-2} to form a cylindrical disc of diameter about 0.6 cm and thickness about 0.1 cm. The current *I* for a series of applied voltages *V* were recorded using a digit multimeter M 3800.

RESULTS AND DISCUSSION

Analytical data: Pyridine of the continuum the proposed compositions are encapsulated into the host supramolecular complexes **I** and **II** to form brown to red charge transfer molecular composites **1–12** depending on the degree of charge transfer. The elemental analysis results reveal that all donor molecules can encapsulate within the

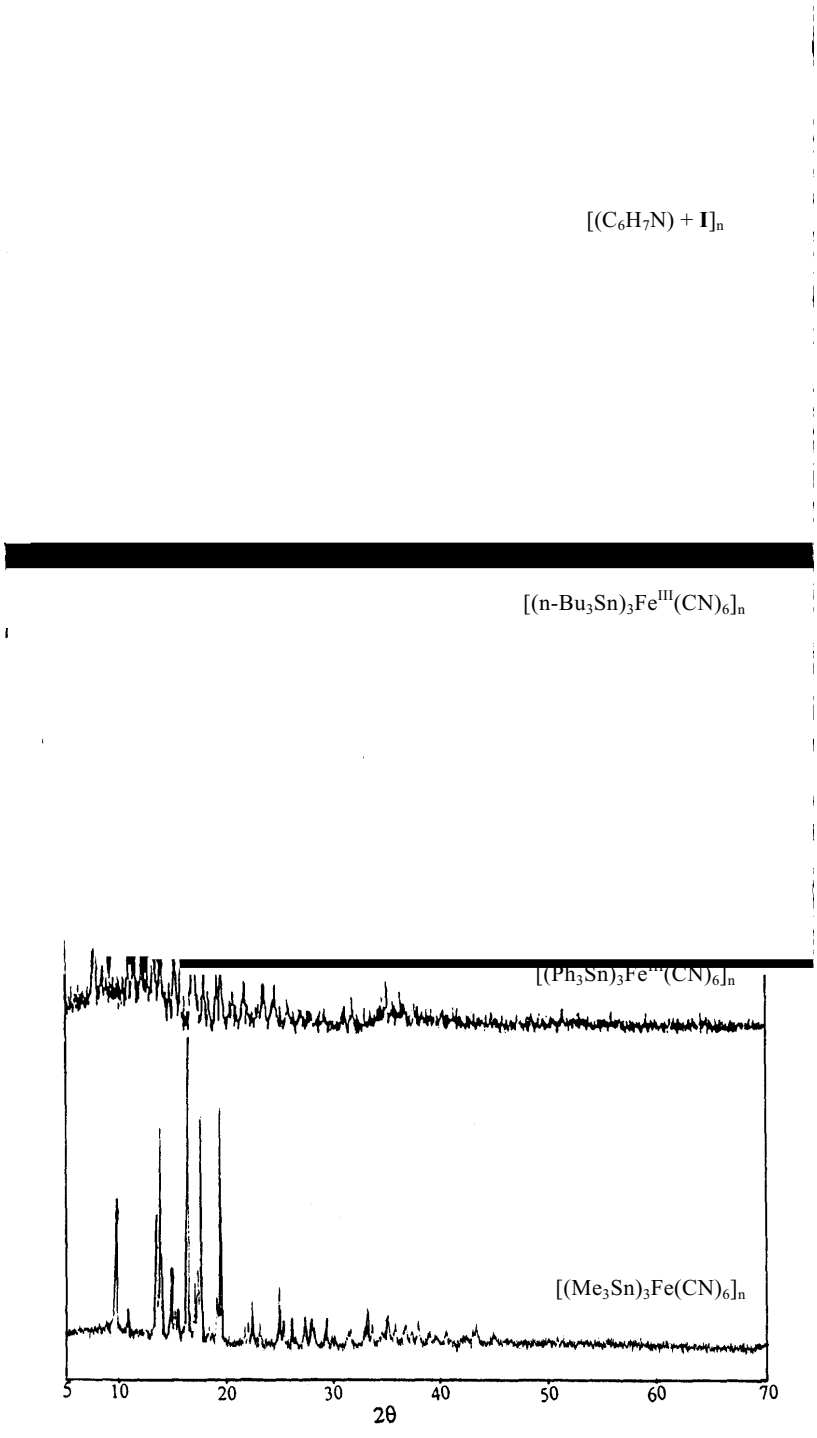

Figure 1. X-ray powder diffraction of the hosts and molecular composite **2**.

cavities of **I** and **II** with an amount less than 1 mole ($x < 1$) per mole of **I** and **II**, except 2-methylpyridine and 4-methylpyridine. These two compounds react with **I** in the ratio of 1:1(compounds **2** and **4**). These ratios depend on the nature of the pyridine compounds and host supramolecular complexes, on the position of the substituents in the pyridine ring and on the conditions used for the reaction.

X-ray powder diffraction: Host supramolecular complexes **I** and **II** are isostructural compounds with the supramolecular complexes $[(Me_3Sn)_3Fe(CN)_6]_n$ [12] as indicated by the X-ray powder diffraction pattern (Fig. 1). On the other hand, the spectra of molecular composite **2** exhibit intense bands different from that of the hosts due to the formation of isostructural $[(Ph_3Sn)_3Fe^{II}(CN)_6^-]_n$, which was produced due to successfully encapsulation of pyridine compound within the cavities. The other molecular composites show a similar X-ray pattern. These results indicate the presence of 3D neutral networks due to the trigonal bipyramidal tbp [-C≡N-Sn-N≡C-] bridges between the single d-transition metal ions $^dM^{+n}$ [3].

The IR spectra of the hosts and the molecular composites: The IR spectra of **I** and **II** reveal the presence of $[-Fe^{III}(CN)_6]^{3-}$ building blocks and the different R_3Sn con-

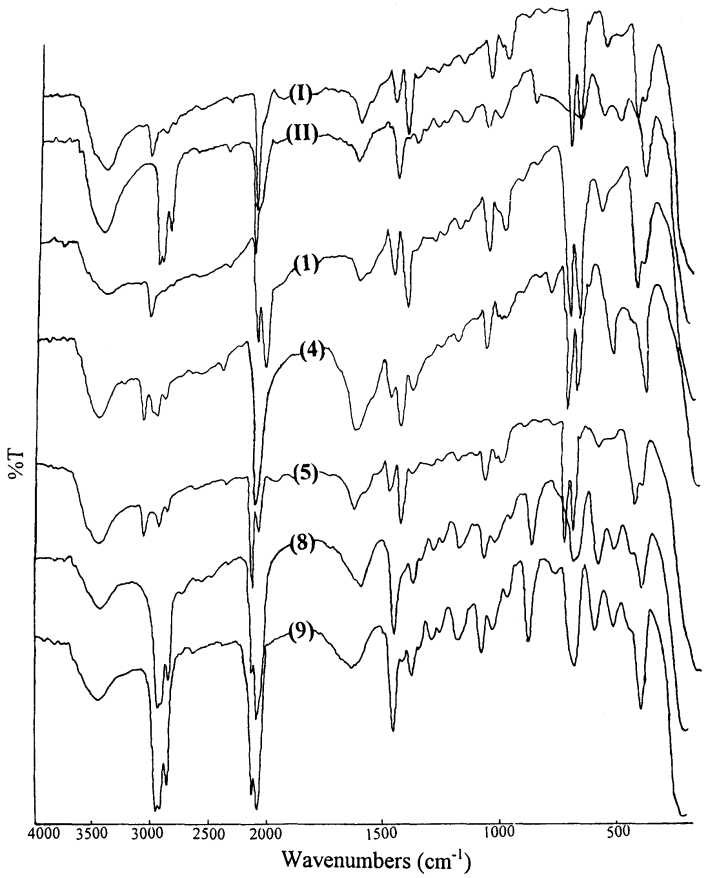

Figure 2. IR spectra of **I** and **II** and the molecular composites **1**, **4**, **5**, **8** and **9**.

necting units (Fig. 2). The IR spectra display strong bands above 2100 cm^{-1}, which correspond to the stretching vibrations of the $[\text{-}Fe^{III}(CN)_6]^{3-}$ building blocks. Both major CN bands are blue-shifted from the stretching vibrations of $[\text{-}Fe^{III}(CN)_6]^{3-}$ in $K_3[Fe(CN)_6]$ (*ca.* $\nu_{CN} = 2105$ cm^{-1}) [3]. Also, the IR spectra of **I** and **II** reveal medium bands at 413 and 401 cm^{-1} and medium bands at 582 and 586 cm^{-1} due to the stretching vibrations of Fe^{III}–C bond and $\nu_{Sn\text{-}C}$, respectively (Table 1). These results reveal the presence of tbp configured $R_3Sn(NC)_2$ units, indicating that these groups play the role of linking the $[\text{-}Fe^{III}(CN)_6]^{3-}$ building blocks and acting as connecting units to form 3D-networks [13].

Table 1. IR spectral data (cm^{-1}) of **I**, **II** and their molecular composites **1–12**.

Compound	ν_{C-H}	$\nu_{C=N}$	$\nu_{C=C}$	$\nu[Fe^{III}CN]$	$\nu[Fe^{II}CN]$	ν_{Sn-C}	$\nu_{Fe^{III}-C}$	$\nu_{Fe^{II}-C}$
I	–	–	–	2140	–	582	413	–
II	–	–	–	2132	–	586	401	–
1	3046	1627	1424	2134	2073	587	413	444
2	3047	1629	1426	–	2068	583	–	447
3	3050	1629	1426	2136	2073	584	412	447
4	3045	1616	1427	–	2062	585	–	449
5	3051	1630	1427	2140	2080	584	414	445
6	3051	1626	1428	2140	2079	582	–	447
7	2955	1615	1456	2130	2084	589	400	421
8	2953	1610	1456	2130	2084	592	403	421
9	2955	1632	1456	2129	2085	597	400	–
10	2955	1630	1456	2128	2085	595	401	421
11	2956	1630	1456	2133	2086	597	401	421
12	2955	1630	1456	2131	2085	597	401	–

The IR spectra of the molecular composites **1–12** reveal the characteristic bands of the corresponding donors and the acceptors (Fig. 2 and Table 1). The IR spectra of **1–12** display medium bands at 2953–3051 cm^{-1} corresponding to ν_{CH}(aromatic) of the pyridine moieties, while those of $\nu_{C=N}$ are located at 1610–1632 cm^{-1}. The IR spectra show also medium to weak bands at 1424–1456 cm^{-1} corresponding to $\nu_{C=C}$ of the pyridine moieties. Generally, the spectra of the pyridine compounds display a shift to lower wavenumbers in the molecular composites due to the presence of charge transfer from the guest pyridine compounds to the host supramolecular complexes. On the other hand, the IR spectra of **I** and **II** exhibit drastic changes on forming molecular composites. A new intense band appears at 2062–2086 cm^{-1} in **1**, **3**, **5–12** due to the stretching vibrations of $[\text{-}Fe^{II}(CN)_6]^{4-}$ building blocks. Medium bands appear at 2140–2128 cm^{-1}, which may be attributed to the stretching vibrations of $[\text{-}Fe^{III}(CN)_6]^{3-}$ building blocks. In addition, the IR spectra of these molecular composites exhibit medium bands in the 400–414 cm^{-1} due to the stretching vibrations of the Fe^{III}–C bond and medium to weak bands at 421–447 cm^{-1} due to the stretching vibrations of the Fe^{II}–C bond. This indicates the partial reduction of Fe^{III} to Fe^{II} by pyridine compounds forming charge transfer molecular composites.

In the case of molecular composites **2** and **4**, the host **I** is completely reduced to the isostructural, $[(Ph_3Sn)_3Fe^{II}(CN)_6^-]_n$ due to the oxidation process. This is facilitated by the donor and acceptor properties of the methyl pyridine compound and the phenyl derivative of the host, respectively. The last process can be corroborated by: (*i*) the disappearance of the bands above 2100 cm^{-1} and at 413 cm^{-1} due to the stretching vibrations of $[\text{-}Fe^{III}(CN)_6]^{3-}$ building blocks and (*ii*) the appearance of intense bands at 2062, 2068, 447 and 449 cm^{-1} due to the stretching vibrations of $[\text{-}Fe^{II}(CN)_6]^{4-}$ building blocks.

Upon encapsulation, the acceptor supramolecular complexes remain having cavities as wide as the donor molecules can accommodate, forming charge transfer molecular composites. This is corroborated from the presence of the medium bands at 582–597 cm^{-1} which are due to the various vibrational modes of the organotin (Sn–C bonds). Therefore, it can be indicated that these groups still play the role of linking $[\text{-}M(CN)_6]^{3-}$ building blocks and acting as connecting units to form 3D-networks [14].

The electronic absorption spectra of the hosts and the molecular composites: The electronic absorption spectra as nujol mull matrix of **I** and **II** exhibit five bands in the region of 220–427 nm (Table 2 and Figs. 3 and 4). These bands are also observed in the absorption spectrum of $K_3[Fe(CN)_6]$ [15]. The first band at 220 nm is due to transitions from the metal to the cyanide ligand (M → L band). The three bands at 260, 300 and 418 or 427 nm have been identified as charge transfer transitions from filled bonding orbitals; mainly of the cyanide ligand, to the hole in the shell of the central metal ion (L → M). The low intense band at 320 nm is due to ligand field (d-d) transitions.

Table 2. The electronic absorption spectral data (nm) of host supramolecular complexes **I** and **II**.

Compound	M → L	L → M CT_1	L → M CT_2	d-d	L → M CT_3
I	220	260	300	320	418
II	–	260	300	320	427

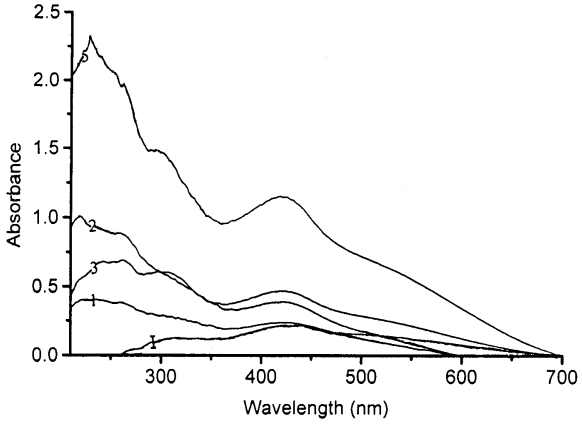

Figure 3. Electronic absorption spectra of **I** and the molecular composites **1**, **2**, **3** and **5**.

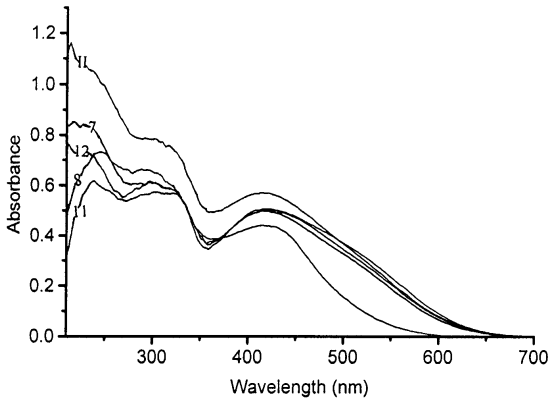

Figure 4. Electronic absorption spectra of **II** and the molecular composites **7**, **8**, **11** and **12**.

The electronic absorption spectra of the molecular composites **1–12** reveal mainly absorption bands in the range 222–421 nm (Figs. 3 and 4 and Table 3). These bands resemble those of pyridine compounds and correspond to the $^1L_a \leftarrow {}^1A$ and $^1L_b \leftarrow {}^1A$ transitions of the phenyl ring of the pyridine compounds [16], in addition to the M $\rightarrow$ L and L $\rightarrow$ M transitions of the host supramolecular complexes. The spectra of the **1**, **3**, **5–12** (with x < 1) reveal a band in the range 414–421 nm due to the L $\rightarrow$ M CT transitions of $[\text{-}Fe^{III}(CN)_6]^{3-}$ building blocks with the appearance of a new band in the range 301–321 nm due to the d-d transitions of $[\text{-}Fe^{II}(CN)_6]^{4-}$ building blocks [13]. These bands support the presence of mixed valence iron due to the partial reduction of Fe^{III} to Fe^{II} as also indicated by the IR spectra of these molecular composites. In the spectra of **2** and **4** (with x = 1), the bands in the range 414–421 nm disappear due to complete reduction of Fe^{III} to Fe^{II} of the host **I** by pyridine compounds. On the other hand, the spectra of **1–12** exhibit an additional broad band at 490–498 nm corresponding to intermolecular charge transfer (CT) transitions from these pyridine compounds to the hosts **I** and **II** [13]. The presence of this band can be considered as good evidence for the encapsulation of pyridine compounds within the cavities of the 3D-supramolecular complexes.

Magnetic properties of the hosts and the molecular composites: The 3D-supramolecular hosts **I** and **II** are obtained as paramagnetic complexes (μ_{eff}; *ca.* 2.036 and 2.18 BM, respectively) due to the presence of low-spin Fe^{III}. On the other hand, the room temperature powder EPR spectra of **I** show broad lines with four g-values 2.2, 2.4, 2.7 and 4.6. These are similar to the behaviour of Fe^{III} ions in $K_3[Fe(CN)_6]$ and some related complexes [17]. The first three bands attributed to low spin Fe^{III}, which has a $(dE)^5$ electronic configuration with one unpaired electron in d_{yz} orbital, forming a distorted octahedral structure with cyanide ions. A weak signal at g 4.6 is also observed due to distorted high spin Fe^{III} [17].

Magnetic measurements of the molecular composites support the spectral data. The molecular composites **1**, **3**, **5–12** are paramagnetic, while **2** and **4** are diamagnetic (Table 4). The magnetic moments of **1**, **3**, **5–12** are characteristic of low-spin Fe^{III}

compounds. The EPR spectra of the paramagnetic molecular composites **1**, **5** and **7** exhibit broad symmetrical signals at g-values 1.6, 2.6, 2.2 and other weak signals at g-values 4.6 and 4.8. The first group of signals correspond to low spin Fe^{III}, while the last signal is known to be characteristic of rhombically distorted high-spin Fe^{III} [9,10]. The presence of the signals in the EPR spectra are good evidence for paramagnetic nature of these molecular composites due to partial reduction of Fe^{III} to Fe^{II} of hosts.

Table 3. The electronic absorption spectral data (nm) of molecular composites **1–12**.

Compound	M → L	L → M CT_1	d-d Fe^{II}–CN	L → M CT_2 Fe^{III}–CN	CT
1	230	259	301	420	495
2	235	258	–	416	490
3	229	257	310	420	490
4	222	250	–	422	490
5	229	255	305	418	497
6	242	261	305	419	498
7	235	279	321	420	498
8	243	249	320	414	495
9	222	250	317	414	495
10	–	240	320	420	490
11	246	262	315	419	495
12	231	260	302	421	498

Table 4. Magnetic moment (BM) and electrical conductivity (S cm^{-1}) at 308 K of the molecular composites **1–12**.

Compound	μ_{eff}	σ	Compound	μ_{eff}	σ
1	3.0	1.6×10^{-2}	**8**	1.8	2.4×10^{-4}
3	2.3	6.0×10^{-3}	**9**	2.2	3.5×10^{-4}
5	2.6	5.6×10^{-3}	**10**	2.4	2.6×10^{-4}
6	3.1	5.8×10^{-3}	**11**	1.9	4.2×10^{-3}
7	2.9	7.1×10^{-3}	**12**	2.2	1.5×10^{-5}

Electrical conductivity of the molecular composites: The molecular composites **1**, **3**, **5–12** are good semiconductors with conductivities in the range of 1.5×10^{-5}–1.6×10^{-2} S cm^{-1} (Table 4). The semiconducting character of these molecular composites was supported by studying the variation of electrical conductivity as a function of temperature (Fig. 5). The dependence of the electrical conductivity on temperature for the molecular composites **1**, **3**, **5–7** satisfies the conventional equation $\sigma = \sigma_0 \exp^{-\Delta E/KT}$, where σ_0 is constant, ΔE is the activation energy and K is the Boltzman's constant. The positive temperature coefficients of electrical conductivity indicate semiconducting character of the molecular composites.

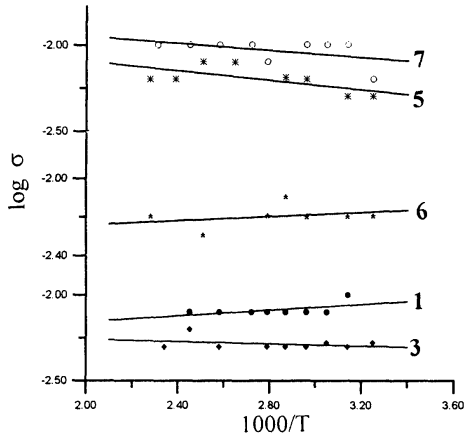

Figure 5. Log σ *vs*. 1000/T for the molecular composites **1**, **3**, **5**–**7**.

REFERENCES

1. Hoskins B.F., Robson R. and Scarlett N.V.Y., *J. Chem. Soc. Chem. Commun*., 2025 (1994).
2. Yünlü K, Höck N. and Fischer R.D., *Angew.Chem., Int. Ed. Engl*., **24**, 879 (1985).
3. Behrens U., Brimah A.K., Soliman T.M., Fischer R.D., Apperley D.C., Davies N.A. and Harris R.K., *Organomet*., **11**, 1718 (1992).
4. Lu J., Harrison T. and Jacobson A., *Inorg. Chem*., **35**, 4271 (1996).
5. Niu T., Lu J., Wang X., Korp J. and Jacobson A., *Inorg. Chem*., **37**, 4271 (1998).
6. Ibrahim A.M.A., Soliman T.M., Etaiw S.H. and Fischer R.D., *J. Organomet. Chem*., **468**, 93 (1994).
7. Ibrahim A.M.A. and Etaiw S.H., *Polyhedron*, **16**, 1585 (1997).
8. Ibrahim M.Sh., *Trans. Met. Chem*., **25(6)**, 695 (2000).
9. Kanamaru E., Shimada M., Koizumi M., Takao M. and Takada T., *J. Solid State Chem*., **7**, 297 (1973).
10. Hagenmuller P., Portier J., Brabe B. and Bouclier P.Z., *Anorg. Allg. Chem*., **355**, 209 (1967).
11. Bonardi A., Carini C., Pelizzi C., Pelizzi G., Predier G., Tarasconi T., Zoroddu M.A. and Molloy K.C., *J. Organomet. Chem*., **401**, 283 (1991).
12. Ibrahim A.M.A., *Polyhedron*, **18**, 2711 (1999).
13. Ibrahim A.M.A., Etaiw S.H. and Soliman T.M., *J. Organomet. Chem*., **430**, 87 (1992).
14. Apperley D.C., Davies N.A., Harris R.K., Brimah A.K., Eller S. and Fischer R.D., *Organomet*., **9**, 2672 (1992).
15. Alexander J.J. and Gray H.B., *J. Am. Chem. Soc*., **90**, 4260 (1968).
16. Etaiw S.E.H., Farag R.S., El-Atrash A.M. and Ibrahim A.M.A., *Spec. Chim. Acta*, **48**, 1025 (1992).
17. Cotton S.A. and Gibson J.F., *J. Chem. Soc*., **A**, 803 (1971).